Analytica Chimica Acta 1299 (2024) 342433

Contents lists available at ScienceDirect

Analytica Chimica Acta

journal homepage: www.elsevier.com/locate/aca

# Addressing the untargeted lipidomics challenge in urine samples: Comparative study of extraction methods by UHPLC-ESI-QTOF-MS

Belen Fernandez Requena [a], Carolina Gonzalez-Riano [a], Coral Barbas [a,*]

[a] Centro de Metabolómica y Bioanálisis (CEMBIO), Facultad de Farmacia, Universidad San Pablo-CEU, CEU Universities, Urbanización Montepríncipe, 28660 Boadilla del Monte, Madrid, España

## HIGHLIGHTS

- Urinary lipidomics aids in studying renal, urological, or endocrine diseases.
- One-phase methods are suitable for obtaining a comprehensive lipidomic profile.
- Analytical reproducibility during sample treatment is crucial in untargeted lipidomics.
- The sample availability is key for selecting the most adequate extraction protocol.

## GRAPHICAL ABSTRACT

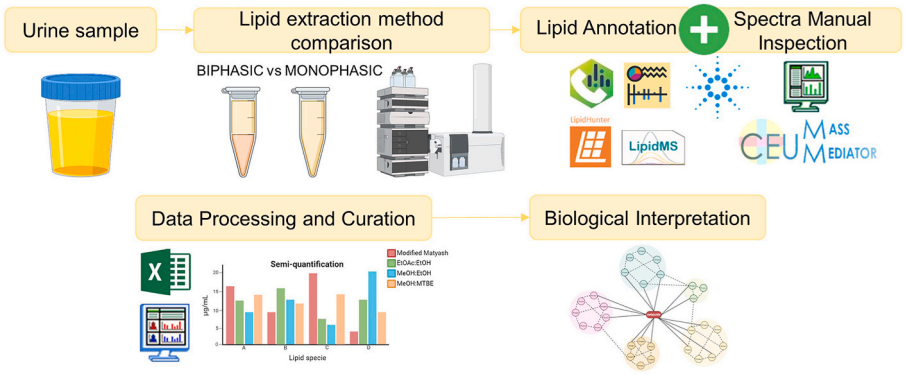


## ARTICLE INFO

Handling editor: L. Liang

*Keywords:*
Urine
Lipidomics
Lipid extraction
Semi-quantification
One-phase method
Biphasic method

## ABSTRACT

Urine analysis has remained a fundamental and widely used method in clinical diagnostics for over a century. With its minimal invasive nature and comprehensive range of analytes, urine has established itself as a clinical diagnostic tool for various disorders, including renal, urological, metabolic, and endocrine diseases. Furthermore, urine's unique attributes make it an attractive matrix for biomarker discovery, as well as in assessing the metabolic and physiological states of patients and healthy individuals alike. However, limitations in our knowledge of average values and sources of urinary lipids decrease the wider clinical application of urinary lipidomics. In this context, untargeted lipidomics analysis relies heavily on the extraction and analysis of lipids in biological samples. Nevertheless, this type of analysis presents challenges in lipid identification due to the diverse nature of lipids. Therefore, proper sample treatment before analysis is crucial to obtain robust and reproducible lipidomic profiles. To address this gap, we conducted a comparative study of a urine pool sample collected from twenty healthy volunteers using four different lipid extraction methods: one biphasic and three monophasic protocols. The extracted lipids were then analyzed using UHPLC-MS and MS/MS, and the semi-quantification of all the accurately annotated lipid species was performed for each extraction method.

* Corresponding author.
*E-mail address:* cbarbas@ceu.es (C. Barbas).

https://doi.org/10.1016/j.aca.2024.342433
Received 13 September 2023; Received in revised form 23 February 2024; Accepted 26 February 2024
Available online 2 March 2024

## 1. Introduction

Urine is a versatile diagnostic medium routinely used to detect a wide range of disorders, including renal, urological, metabolic, and endocrine diseases. Clinical diagnostic tools have been established to analyze cells, cellular fragments, electrolytes, metabolites, and proteins qualitatively and quantitatively in urine, providing valuable information for accurate diagnosis and treatment. Depending on the biological matrix, some sample-collecting protocols could result in highly invasive procedures involving patient issues and risks. It also increases the difficulty of the experimental design and diminishes the possibility of including healthy control groups in the study due to the clear refusal of volunteers to undergo these procedures. As a minimally invasive and easily accessible sample, urine plays a crucial role in modern medicine as an effective diagnostic tool with easy handling and storage [1,2]. Moreover, urine is a perfect source for determining specific disease biomarkers, pharma drug metabolism monitoring, and toxicity tests.

The current knowledge of the crucial role played by lipid metabolic homeostasis in maintaining normal physiological conditions highlights the significance of lipidomics analysis as an essential research discipline for detecting lipid metabolic imbalances responsible for various diseases [3]. Recent research has focused on developing a lipidomic methodology to enable early diagnosis, monitoring, and treatment control of acute and chronic kidney diseases (CKD) [4]. However, our understanding of urinary lipidomic changes in CDK remains limited. Although urinary lipids have been proposed as a diagnostic tool, promising biomarkers such as phospholipids have been identified for early detection of breast and prostate cancer. In addition, recent studies have demonstrated the potential of lipid mediator profiling in urine as a non-invasive approach for molecular phenotyping of asthma and atopic dermatitis diagnosis [5]. These findings suggest the potential for utilizing urine lipidomic profiling for biomarker discovery in diverse pathologies, providing valuable insights into disease pathogenesis and aiding in personalized treatment strategies. However, limitations to the broader clinical application of urinary lipidomics exist due to our limited knowledge of average values and sources of urinary lipids.

In this regard, liquid chromatography coupled with mass spectrometry (LC-MS)-based untargeted lipidomics is a widely used analytical technique to perform lipidomics analysis for clinical studies [6,7]. Typically, the two main steps in which we can summarize lipidomics studies are the extraction and analysis of lipids, followed by the annotation/identification and quantification of those lipids present in the biological samples. Lipidomics analysis could be performed following either a targeted or an untargeted approach. An untargeted approach can maximize the detection of most lipid classes, producing a more detailed lipidomic profile that may even detect previously unknown lipid species [8,9]. However, it can also increase the difficulty of proper lipid identification due to the complexity of this diverse family of biomolecules, which presents a challenge in obtaining high lipid recovery rates during extraction [10–12]. As such, proper sample treatment before analysis is crucial for obtaining a robust and complex lipidomic profile, as emphasized in previous studies [10,13,14].

Biphasic lipid-lipid extractions such as Folch [15], Bligh and Dyer [16], or Matyash [17] have been broadly used for lipidomics studies. So far, different modifications of these methods have appeared for specific applications but keep the basis of these extractions [18]. In contrast, monophasic extraction methods have gained popularity over the past decade as they simultaneously enable the analysis of both polar and nonpolar metabolites. These methods are preferred over biphasic extractions due to their less complex application [19] and more importantly, due to the fact that more polar lipids are not split into the two phases. In the literature, there are multiple reports comparing different extraction methods for plasma samples. However, as urine is a more polar matrix, other comparative studies must be conducted for untargeted lipidomics using urine samples. To address this gap, we conducted a study in which we extracted lipids from ten independent aliquots collected from a urine pool sample composed of twenty healthy volunteers. Four different methods were used for lipid extraction, including one biphasic method and three monophasic methods. We then measured the samples using UHPLC-MS and MS/MS to obtain the lipid landscape of urine, covering the wider range of lipid classes and species as our main goal. Finally, we performed the relative quantification of the detected lipid species by each extraction method (Fig. 1). By using multiple protocols, we observed that all of them provided the same number of lipid species. Consequently, we focused on the analytical reproducibility of each extraction protocol to identify the optimal approach for untargeted lipidomics in urine samples.

## 2. Materials and methods

### 2.1. Reagents and lipid standards

Ethyl acetated (EtOAc) and ethanol (EtOH) for lipid extraction were obtained from VWR International SAS (France). The ammonium fluoride ($NH_4F$) (ACS reagent, ≥98%) and Methyl-tert-butyl ether (MTBE) were purchased from Sigma-Aldrich (Steinheim, Germany). LC-MS grade methanol (MeOH), acetonitrile (ACN), and isopropanol (IPA) were obtained from Fisher Scientific (Pennsylvania, United States). Ammonia solution (28%, GPR RECTAPUR®) and acetic acid glacial (AnalaR®NORMAPUR®) were obtained from VWR Chemicals (Pennsylvania, United States). Reverse-osmosed ultrapure water, used to prepare all the aqueous solutions, was obtained from a Milli-Qplus185 system (Millipore, Billerica, MA, USA).

For lipid quantification and analytical quality assurance, SPLASH® Lipidomix®, $C_{17}$ – Sphinganine and $d_{31}$–palmitic acid was purchased from Avanti Polar Lipids (Alabaster, Alabama, USA). The compositions of applied internal standard mixtures are listed in Table S1.

### 2.2. Urine samples

A pool of urine samples collected from twenty healthy volunteers was employed for this study, divided into eight males (mean age 30.0 ± 12.1SD, mean weight 75.6 ± 7.7SD) and 12 females mean age 28.1 ± 10.9SD, mean weight 63.4 ± 8.4SD). Urine samples were prepared at the "Centro de Metabolómica y Bioanálisis, CEMBIO" (Madrid, Spain), following four different extraction methods to obtain the urine lipidomics fingerprint. Briefly, the samples were thawed on ice and then vortex-mixed for 2 min. Next, 150 μL of urine was collected from each sample to generate the urine pool sample. Finally, we took the specific volume for each one of the fourth analytical methods tested necessary for the lipid extraction. We prepared ten replicates for each extraction method, which were treated following the different lipid extraction protocols. A mixture of nonendogenous internal standards (Table S1) was added before performing the four extraction procedures.

#### 2.2.1. Two-phase extraction method

*2.2.1.1. Modified Matyash extraction method [20].* On the ice, 20 μL of urine pool sample was mixed with 225 μL of cold (−20 °C) MeOH. Afterwards, samples were vortex-mixed for 30 s, followed by the addition of 750 μL of MTBE. Samples were vortex-mixed again for 6 min, and 188 μL of Ultra-Pure MilliQ® water was added. Samples were then vortexed for 1 min. After centrifugation for 2 min at 16.1 rpm at 15 °C, 300 μL of supernatant was carefully recovered and dried in a SpeedVac for 2 h at 45 °C. Finally, samples were resuspended in 100 μL of MeOH:MTBE (1:1, v/v) before the UHPLC-MS analysis.

#### 2.2.2. One-phase extraction methods

*2.2.2.1. Method 1 – ethyl acetate:Ethanol (EtOAc:EtOH) (2:1, v/v).* On the ice, 10 μL of urine pool sample was mixed with 800 μL of a cold

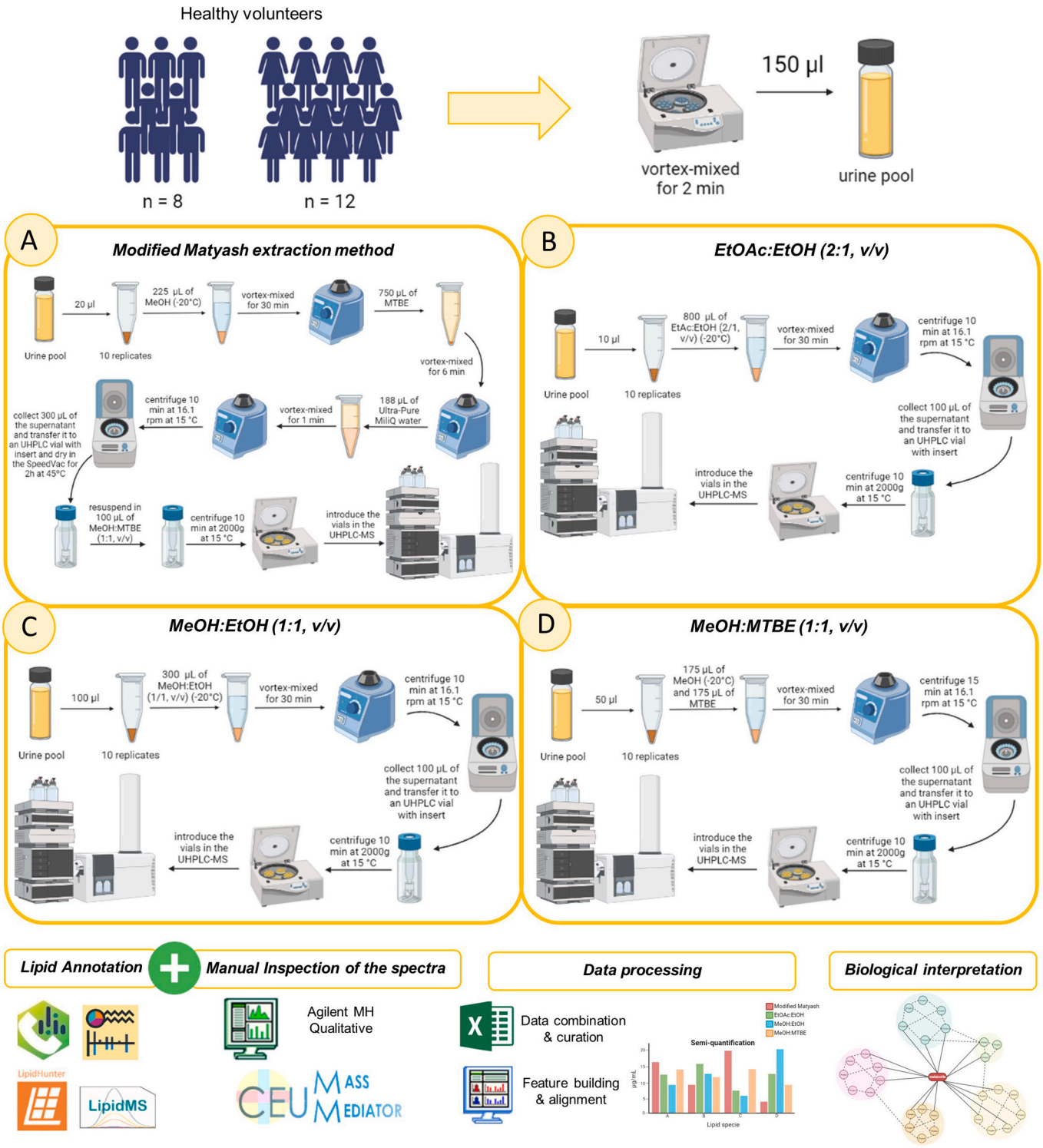


**Fig. 1.** Workflow of the analytical procedure and data processing carried out in this study.

(−20 °C) mixture of EtOAc and EtOH (2:1, v/v). Samples were vortex-mixed for 30 min and then centrifuged for 10 min at 16.1 rpm at 15 °C. Finally, 100 µL of supernatant was collected and transferred into an HPLC-MS vial with a glass insert.

*2.2.2.2. Method 2 – Methanol:Ethanol (MeOH:EtOH) (1:1, v/v).* On the ice, 100 µL of urine pool sample was mixed with 300 µL of a cold (−20 °C) mixture of MeOH:EtOH (1:1, v/v). Samples were vortex-mixed for 30 min. After centrifugation for 10 min at 16.1 rpm at 15 °C, 100 µL of the supernatant was collected and transferred into an HPLC-MS vial with a glass insert.

*2.2.2.3. Method 3 – Methanol:Methyl tert-butyl ether (MeOH:MTBE) (1:1, v/v).* On the ice, 50 µL of urine pool sample was mixed with 175 µL of cold (−20 °C) MeOH and 175 µL of MTBE. Samples were then vortex-mixed for 30 min. After centrifugation for 15 min at 16.1 rpm at 15 °C, 100 µL of the supernatant was collected and transferred into an HPLC-MS vial with a glass insert.

Finally, all the vials were centrifuged at 2000g at 15 °C for 10 min before injecting into the system. Following the same lipid extraction protocols, four blank samples—one for each extraction method—were generated alongside the others. The blank samples were then analyzed at the beginning and end of the analytical run to identify common contaminations.

The analysis of urine extracts was performed on an Agilent 1290 Infinity II UHPLC system coupled to an Agilent 6545 quadrupole time-of-flight (QTOF) mass spectrometer in both positive and negative ion modes using the analytical conditions previously described [21].

### 2.3. Lipidomics analysis

#### 2.3.1. Analytical conditions selected for a lipidomics analysis

We performed an untargeted lipidomics analysis to cover the broader spectrum of urine lipidome. The analytical platform selected for data acquisition was an Agilent 1290 Infinity II Ultra-High-Performance Liquid-Chromatography (UHPLC) system coupled to an Agilent 6546 quadrupole time-of-flight (QTOF) mass spectrometer. The Agilent 1290 Infinity II Multisampler system was used to uptake 1 μL of extracted samples, maintaining the temperature at 15 °C to preserve compounds and avoid lipid precipitation. We used an Agilent InfinityLab Poroshell 120 EC –C18 (3.0 × 100 mm, 2.7 μm) (Agilent Technologies) column and a compatible guard column (Agilent InfinityLab Poroshell 120 EC –C18, 3.0 × 5 mm, 2.7 μm), both held at 50 °C.

The parameters of the Agilent 6546 QTOF mass spectrometer equipped with a dual AJS ESI ion source were: 150 V fragmentor, 65 V skimmer, 3500 V capillary voltage, 750 V octopole radio frequency voltage, 10 L/min nebulizer gas flow, 200 °C gas temperature, 50 psi nebulizer gas pressure, 12 L/min sheath gas flow, and 300 °C sheath gas temperature. Data were collected in positive and negative ESI modes in separate runs, operated in full scan mode from 40 to 1700 *m/z* with a scan rate of 3 spectra/s. A solution consisting of two reference mass compounds was used throughout the whole analysis: purine (C5H4N4) at *m/z* 121.0509 for the positive and *m/z* 119.0363 for the negative ionization modes; and HP-0921 (C18H18O6N3P3F24) at *m/z* 922.0098 for the positive and *m/z* 980.0163 (HP-0921 + acetate) for the negative ionization modes. These masses were continuously infused into the system through an Agilent 1260 Iso Pump at a 1 mL/min (split ratio 1:100) to provide a constant mass correction.

The mobile phases used for both ionization modes, positive and negative, consisted of (A) 10 mM ammonium acetate, 0.2 mM ammonium fluoride in 9:1 water/MeOH and (B) 10 mM ammonium acetate, 0.2 mM ammonium fluoride in 2:3:5 acetonitrile/MeOH/isopropanol. The multiwash strategy consisted of a solvent mixture of methanol:isopropanol (50:50, v/v) with a wash time set at 15 s and an aqueous organic phase (30:70, v/v) mixture to assist in the starting conditions. The chromatography gradient started at 70% of B at 0–1 min, 86% at 3.5–10 min, and 100% B at 11–17 min. Starting conditions were recovered at minute 17, followed by a 2 min re-equilibration time, a total running time of 19 min. The flow rate during the analysis was kept constant at 0.6 mL/min.

Iterative-MS/MS acquisition modes were performed for both ion modes, positive and negative. We performed ten measurements of a selected sample using two different collision energy, 20 eV and 40 eV. The software selects the three more intense precursor ions for each measurement, which were fragmented to obtain the spectrum for a specific time. In the subsequent measurement of the same sample, for the same specific time point, the software excluded the previous three selected ions and selected the following three more intense precursor ions. By measuring the sample several times, we obtained thousands of MS/MS spectrums at the end, covering most of the lipidome spectrum.

#### 2.3.2. Lipid annotation process

Lipidomics studies face a significant challenge in accurately annotating and identifying the complete lipidome of biological samples. Researchers have made notable progress by developing various bioinformatic tools to overcome this bottleneck to obtain a more comprehensive lipid profile. In our study, we tackled this issue by devising a custom strategy for lipid annotation, integrating four software tools based on three distinct annotation strategies. Further insights into the performance of these tools, their limitations, and the exclusion criteria applied in our annotation approach are detailed in the previously published work by B. Fernández Requena et al. [22]. This approach enhanced the accuracy and scope of lipid annotation in our analysis. The software parameters were set as follows.

- *Lipid Annotator v1.0* (Agilent): Q-Score ≥20.0, adduct selection $H^+$, $Na^+$ and $NH_4^+$ for positive ion mode and $H^-$ and $C_2H_3O_2^-$ for negative ion mode. We selected all lipid classes to perform an untargeted analysis. For the ID parameters, the Mass Threshold was set at mass deviation ≤20.0 ppm, the "Report top candidate only" option was selected, the Fragment score was ≥30, the Total score was ≥60, and the Constituent Level was ≥10%.
- *MS-DIAL 4* (Riken): the raw data files were converted into "*.ibf*" files using the MS IBF file Converter software. For MS/MS data reprocessing, we selected the soft ionization for LC-MS/MS, chromatography separation type, conventional LC-MS method type, and profile data as the data type. We selected the corresponding ionization mode (positive or negative) for each analysis and Lipidomics as the target omics. The MS1 and MS/MS *m/z* detection window was set at 40–1700 Da, and the retention time window was set at 0–19 min. The peak detection window, smoothing level was set as 1 scan. The Accurate mass tolerance was 0.01 Da for MS1 and 0.025 for MS2 for the Identification window, and the identification score cut off was set at 70%. Next, we selected specific adducts depending on the ionization mode that we were analyzing ($H^+$, $Na^+$ and $NH_4^+$ for positive and $H^-$ and $C_2H_3O_2^-$ for negative ion mode). The rest of parameters were set as default.
- *LipidHunter*: we set from 0 to 19 min the scan range, 40–1700 *m/z* range, ± 0.75 *m/z* precursor window, DDA Top 6, ± 20 ppm for MS tolerance level, the absolute intensity for the MS level threshold was set at 1000, ± 20 ppm MS/MS tolerance level, the absolute intensity for the MS/MS level threshold was set at 10, 80% isotope score, 75% Rank score and 0.10% as the minimum relative intensity for the scoring.
- *LipidMS 3.0:* We reprocessed our data by selecting the Batch processing option in the corresponding ionization mode. The *m/z* tolerance for MS1 and MS/MS was set at 20 ppm. The tolerance for the RT window was set at 300 s. The rest of the parameters were set as default. Finally, the lipid classes selected for the annotation process were established according to the ionization mode.

Afterwards, the information obtained was combined and manually curated to remove redundancy and false positive annotations. Furthermore, we manually inspected the MS/MS data from both positive and negative ionization modes to increase confidence in the annotations provided. The process was supported using the CEU Mass Mediator free access tool [23].

#### 2.3.3. Data reprocessing

To determine the differences in the urine lipidomic profile obtained through the different extraction methods, we reprocessed our raw data files using the Agilent MassHunter Profinder software (B.10.0.2, Agilent Technologies, Santa Clara, CA, USA), using the "Batch Targeted Feature Extraction" mode to perform the feature extraction and time alignment. The data matrix employed for the feature extraction and time alignment included the molecular formula, exact mass, and retention time. Features were built as the sum of coeluting ions related by charge-state envelope, isotopologue pattern, and/or the presence of different adducts and dimers in the analyzed samples. The following adducts were selected to detect coeluting adducts of the same feature: $[M+H]^+$,

$[M+Na]^+$, $[M+K]^+$, $[M + NH4]^+$ and $[M + C2H6N2+H]^+$ for positive ionization mode; $[M - H]^-$, $[M+Cl]^-$, $[M + CH3COOH-H]^-$, and $[M + CH3COONa-H]^-$ for negative ionization.

The isotope grouping was set to common organic molecules, and the charge state was limited to 1–2. The match tolerance was set at ± 20 ppm for masses and ± 0.500 min for retention times. The retention time score contribution to the overall score was 100.00. In the matching criteria options, we selected "warn if scores are" < 75.00 for low score matches and "warn if the second ion's abundance is" > 50.00 for single ion matches. The integration was made with "Agile 2". As peak filters, we selected peak height and the limit of the maximum number of peaks was set to 5. The chromatogram data format was Centroid. The parameters for peak spectrum were: average scans >10% of peak height, TOF spectra were excluded if above 20.0 % of saturation in the *m/z* ranges used in the chromatogram and never returned an empty spectrum. For centroiding, the peak location was set at two as maximum spike width and 0.70 required valleys, and the mass spectral data format was Centroid. Finally, as post-processing filters, a feature must be present in at least 50% of the samples in at least one sample group.

#### 2.3.4. Data normalization and pre-processing

First, data were normalized and filtered to ensure data quality. The raw data matrices were then normalized using the SPLASH® Lipidomix® mixture. For the normalization process, the adduct with which each lipid species was detected was considered. This adjustment involved comparing the signal detected for that specific adduct with the signal detected for the same adduct in the corresponding lipid species found in the SPLASH® Lipidomix® mixture to account for unwanted variance due to sample preparation and the analytical run. Features with mean blank values above 10% of the mean value in the samples were removed. Additionally, we proceed to study the reproducibility of the different lipid extraction methods. For this purpose, the coefficient of variation (CV) of each annotated lipid species was calculated. Next, the average and standard deviation of the CV of each extraction method in each lipid class were calculated. The obtained data are listed in Table S2. Afterwards, the concentration of the annotated lipids obtained with each method was plotted to study each extraction method's performance for each lipid class. The plots were generated using GraphPad Prism software (v9.0). The error bars displayed in the graphics represented the standard error of the mean (SEM).

#### 2.3.5. Semi-quantification of the lipid species detected

One of the most significant challenges when performing a non-targeted lipidomics-based approach is the quantification of the analytes of interest. The addition of the SPLASH® Lipidomix® standard mixture, which contains nonendogenous class-specific lipid standards, together with the C17-Sphinganine, and d31-palmitic acid mixture allowed the quantification of 18 lipid subclasses by assuming that each lipid standard has the same response factor (RF) as the lipid of interest belonging to that class [24]. The rest of the detected lipids were semi-quantified using the standard that presented the minimum difference in RT and mass with the biological compound [24]. Furthermore, we have assessed the recovery efficiency of individual extraction methods by comparing the areas of each lipid standard present in the SPLASH® Lipidomix® standard mixture added to the sample compared to a reference standard. This comparison was conducted using a solvent sample, including the SPLASH® Lipidomix®, and the same standards added to each sample in each extraction method (Table S3).

## 3. Results and discussion

### 3.1. Lipid annotation strategy

Selecting the most appropriate lipid extraction method is a crucial step in the elucidation of the complete lipid profile of a biological matrix [20]. To address the need for comparative and quantitative lipid extraction studies for untargeted lipidomics using urine samples [19], we tested four lipid extraction methods: one biphasic method and three monophasic methods. Our main goal was to determine the best solvent combination to maximize the coverage of lipid species displayed in the urine.

Attempting to provide a confident structure characterization of the lipid species detected, a parallel acquisition of HRMS and MS/MS data using Data-dependent analysis (DDA) at two fixed collision energies (20 eV and 40 eV) was performed. Afterwards, the data files obtained from the MS and MS/MS acquisition modes, for both positive and negative ionization modes, were processed using different annotation strategies to increase the coverage and precision of the annotation. Those strategies were based on the spectral matching with the internal in silico libraries of Lipid Annotator [25] and MS-Dial [26] software tools, the bottom-up strategy with a predefined fatty acid checklist included in LipidHunter [27] and the last one, based on the fragmentation patterns and the intensity rules of the fragments by using LipidMS [28,29] software. The tentative annotation list obtained from the software programs was curated to delete duplicates and false positives. Additionally, the MS and MS/MS raw data files were manually inspected using the MassHunter Qualitative v10.0 and the CEU Mass Mediator free access tool [23] to increase the accuracy of the annotation process. Thanks to the manual inspection, we were able to detect the precursor ion *m/z* (MS1), and the specific fragmentation pattern spectrum (MS2) of each lipid, which provide enough structural information to assign the exact lipid class, the molecular species, the degree of unsaturation and the fatty acid chain position [30,31]. As an additional checkpoint in curating the lipid annotations, we also introduced the retention time (RT) mapping to define the elution order using the Kendrick mass defect (KMD) plots. This approach led to a more comprehensive analysis of the samples and provided more accurate and reliable results.

Thanks to this annotation workflow, we could correctly annotate 315 lipid species (Table S4) divided into four main lipid classes: sphingolipids (SP), glycerophospholipids (GP), glycerolipids (GL) and fatty acyls (FA) and eighteen different lipid subclasses (Fig. 2). The annotated lipids were classified using the LIPIDMAPS classification system [32].

After MS data reprocessing using the Batch Targeted Feature Extraction mode of the Agilent MassHunter Profinder software, 415 and 192 features were obtained in ESI (+) and ESI (−), respectively. After data normalization and filtration, the resulting data matrices displayed 283 features for ESI (+) and 179 for ESI (−). Ultimately, a total of 315 distinct lipid species were successfully annotated after data combination, curation, and manual inspection of the data, reflecting the urine lipid landscape composition and the abundance of each lipid compound present in the healthy urine samples. Fig. 3A illustrates the number of lipid species annotated with each software tool and the degree of overlap using a Venn diagram. MS-DIAL exhibited the highest performance of the software tools, successfully annotating 206 lipid species. Following closely, the Lipid Annotator identified 154 lipid species, but only 53 overlapped with the results from MS-DIAL. Similarly, LipidHunter and LipidMS annotated 103 and 100 lipid species, respectively, with only 7 species being common between both programs. Notably, the overlap among the annotation results obtained from the different software tools was minimal, with only 24 lipid species being annotated by all four programs. This highlights the complementary nature of annotation libraries and the importance of carefully considering the annotation strategy to prevent potential bias when interpreting data. Finally, 22 lipid species were successfully annotated thanks to the careful manual inspection of the MS and MS/MS data. This process was performed to unveil new lipids and enhance the reliability and confidence of the lipid annotations performed [22].

Despite the current limited knowledge of typical values, the sources of urinary lipids, and their normal variations in healthy individuals following a regular diet [33], it is established that glomerular filtration and tubular transport mechanisms influence the composition of urinary lipid species. These mechanisms are closely connected to the excretion

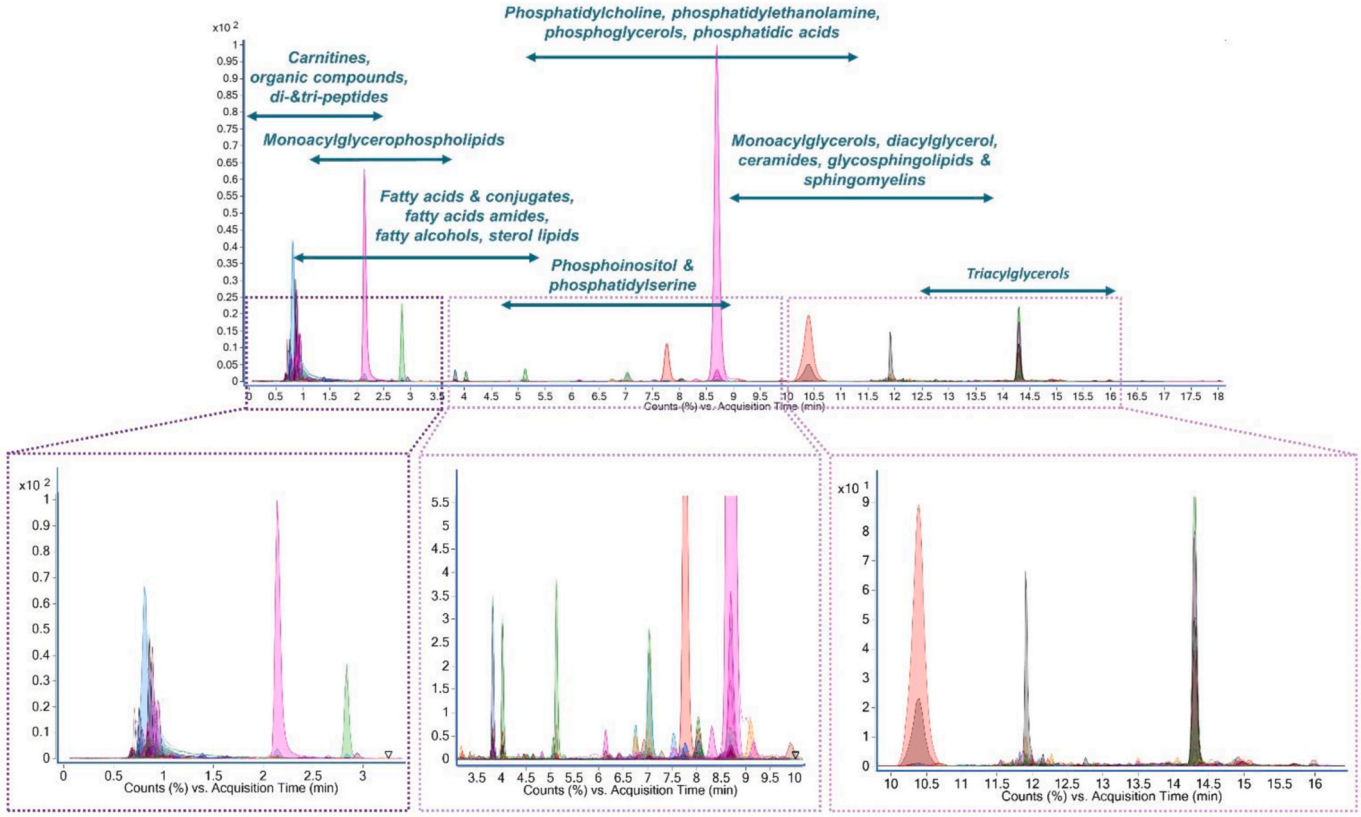


**Fig. 2.** The urinary Total Compound Chromatogram (TCC) presented in this picture revealed the elution times of distinct lipid subclasses during LC-MS analysis, as indicated by the arrows. In the lower section, a magnified view comprehensively explored the less abundant detected lipids.

of urine creatinine and albumin (diuresis) in both men and women. Additionally, in women, the presence of lipid species originating from urinary cells and cellular components has a significant impact on the overall composition of the urine lipidome [4]. In addition, the lipid class proportion present in the urine could be influenced by several factors, including the metabolic state of the organism under study, the analytical conditions and the resolving power of the instrument, the complexity of the biological matrix and the lipid extraction method applied [34]. The last one is the main point of interest in this study. The four extraction protocols used in this work exhibited homogeneous lipid profiles in terms of lipid species composition and the total number of annotated lipids. It demonstrated the efficiency of monophasic extraction methods, which covered the same lipid range as the biphasic method during the extraction procedure. However, the relative abundance of each lipid species differed among the four tested procedures due to the lipid class polarities [19].

In Fig. 3B, depicting the qualitative profile of urine lipid composition, GLs emerged as the dominant lipid class, constituting 30.0% of the total urinary lipid content. Triacylglycerols (TGs) were the most abundant subclass within the glycerolipids, accounting for 20.0% of the overall lipid content in urine. GPs were also significant components, comprising 29.5% of the overall urinary lipid composition. Glycerophosphocholines (PC) and glycerophosphoethanolamines (PE) were found in notable amounts, constituting 15.0% and 5.0% of the glycerophospholipid content, respectively. SP constituted 22.0% of the total lipid content, where ceramides (Cer) and sphingomyelins (SM) were almost equally abundant, SM being slightly more prevalent by 1%. Furthermore, fatty acyls were present in the urine lipid composition, accounting for 18.0% of the total content. Among the fatty acyls, fatty acylcarnitines (Car) represented the most significant proportion at 8.0%, followed by fatty acids (FA) at 6.0%, hydroxy-fatty acids (FA (OH)) at 3.0%, and fatty esters (FAHFA) at 1.0%. The composition landscape within each lipid class, in terms of aliphatic chain composition and the degree of unsaturation, is depicted in Fig. 3C. This comprehensive analysis provides insights into the diverse lipid profile in urine and highlights the relative abundances of various lipid classes and subclasses.

It must be kept in mind that DDA is a procedure conducted by an automated instrument that dynamically selects the top precursors and fragments them. This process introduces some inherent bias. A notable limitation of DDA is that less abundant signals may remain unanalyzed and thus unidentified in the experiment. Oxylipins are bioactive lipid mediators crucial in various physiological processes, such as blood flow regulation and inflammation. However, the analysis of oxylipins presents significant challenges, mainly due to their limited presence in samples, structural diversity, and stability. Therefore, effective sample preparation methods are required to extract, purify, and concentrate the target eicosanoids from urine while removing potential interfering substances [35]. As a result, the software tools used in our study could not annotate this compound class due to their low biological abundance. Most of these oxylipins fell below the noise threshold set in the DDA analysis. Consequently, manual data inspection became necessary, leading us to annotate only two oxylipins successfully, 8-iso-15--keto-PGF2α (Fig. 4A) and 11-dehydro-TXB3 (Fig. 4B). 8-Iso-15--keto-PGF2α is a prostaglandin commonly used as a biomarker for oxidative stress in various physiological and pathological conditions. It is considered a reliable indicator of oxidative damage to cell membranes and tissues, as it is produced during lipid oxidation. Elevated levels of 8-iso-15-keto-PGF2α in biological samples, such as urine or blood, can indicate increased oxidative stress associated with multiple inflammation oxidative stress-related disorders, including cardiovascular diseases, asthma, chronic obstructive pulmonary disease, interstitial lung disease, cystic fibrosis, or acute chest syndrome [36]. On the other hand, 11-dehydro TXB3 has been described as a urinary metabolite of TXA3 in

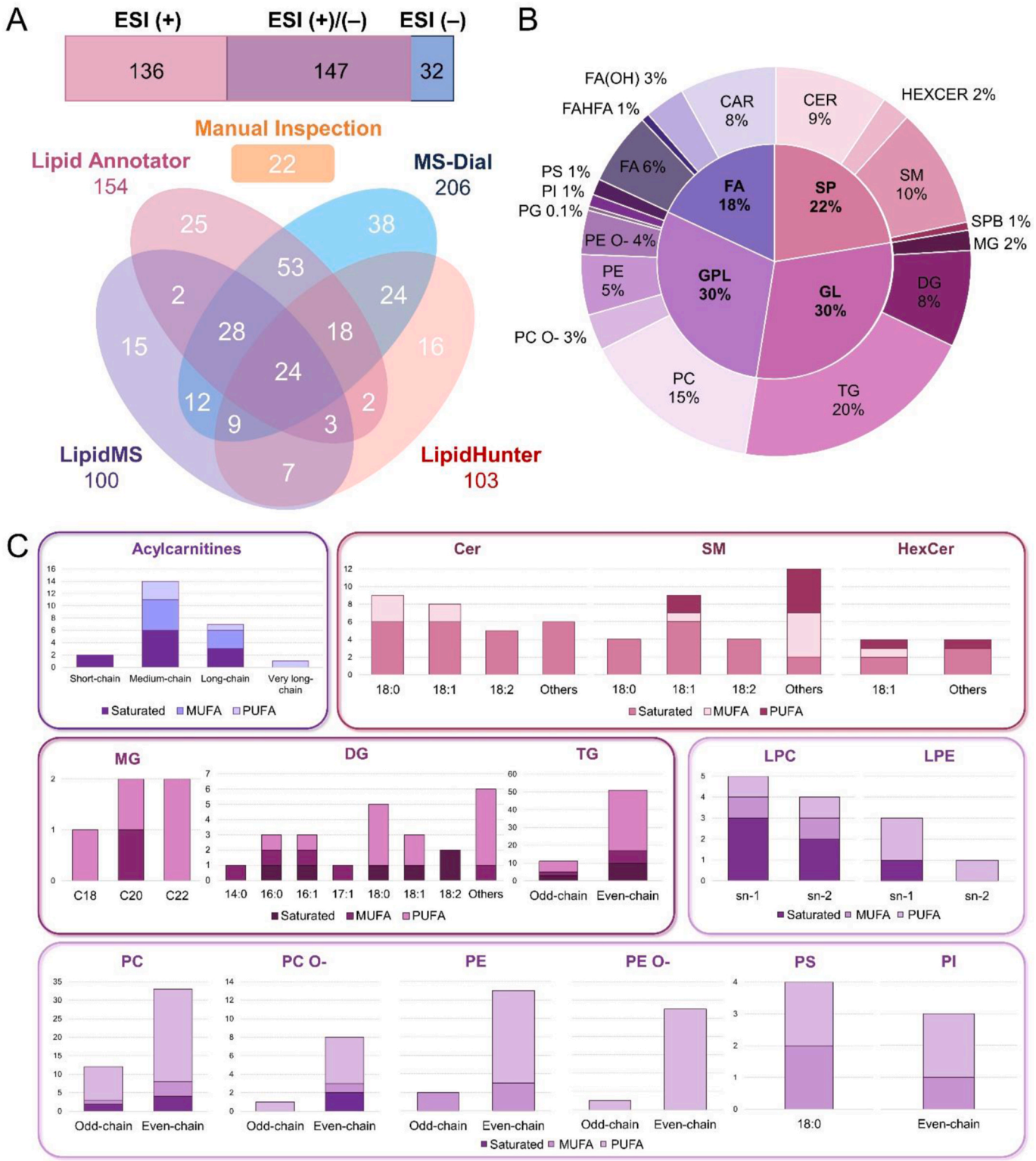


**Fig. 3.** **(A)** Number of high-quality features considered in both ESI(+) and ESI(−) ion modes after data curation. Additionally, the Venn diagram depicts the overlapping number of the lipid species annotated using different automated annotation tools. **(B)** Circular qualitative diagram of the lipidomic landscape detected in healthy urine samples based on the LIPIDMAPS classification system. **(C)** Distribution of the most representative lipid classes detected by aliphatic chain composition and degree of unsaturation. The data obtained relative to glycerophosphoglycerophosphates (PGs) and sphingoid base (SPB) is not shown due to the reduced number of lipid species detected during the lipid annotation.

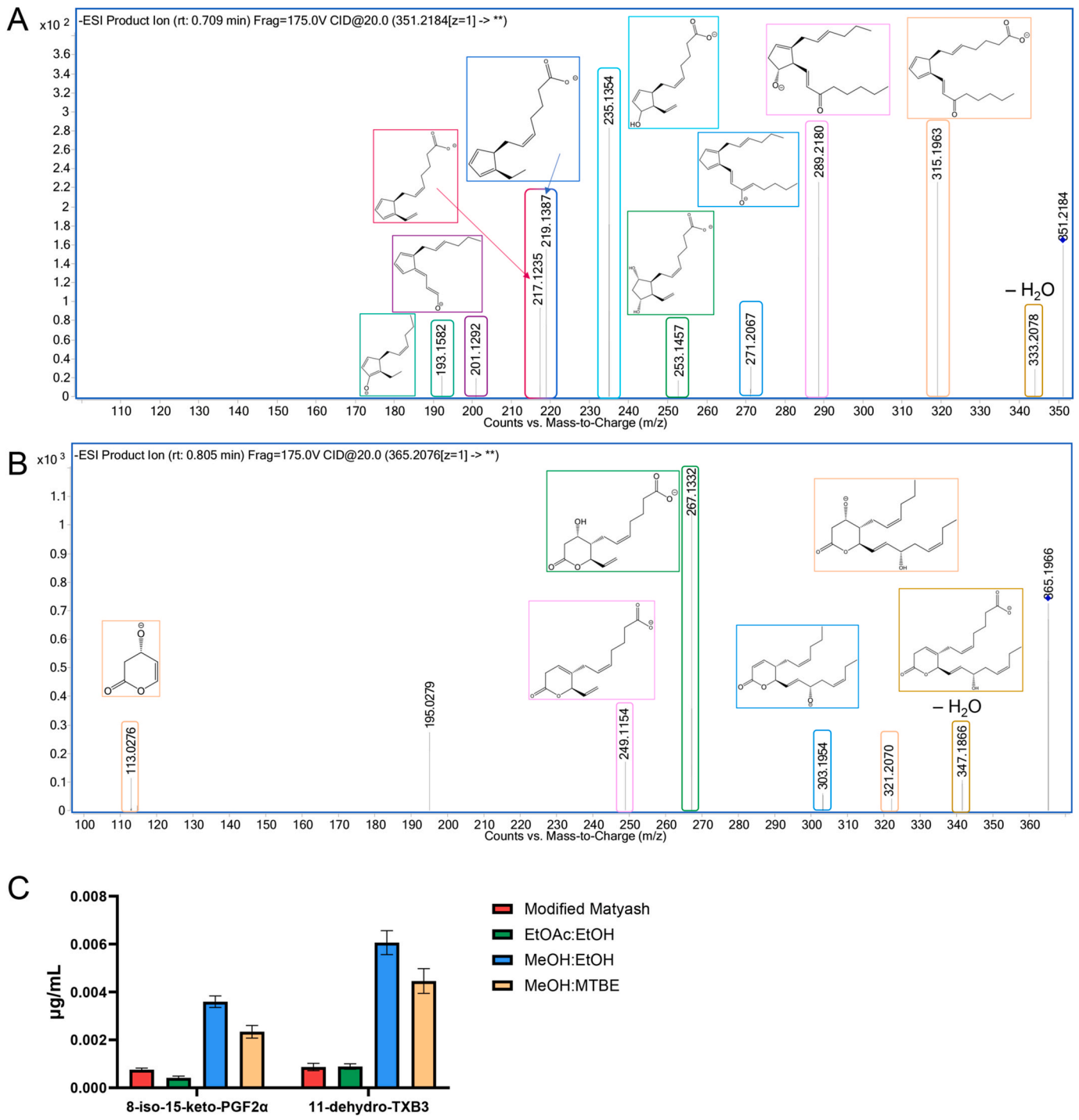


**Fig. 4.** (A) ESI(−)-MS/MS spectrum of 8-iso-15-keto-PGF2α. **(B)** ESI(−)-MS/MS spectrum of 11-dehydro-TXB3. **(C)** Relative quantification of both oxylipins detected in the urine by each extraction method. The error bars displayed are the standard error of mean (SEM).

humans with enhanced dietary intake of EPA [37]. As depicted in Fig. 4C, MeOH:EtOH (1:1, v/v) method extracted the highest amount of both oxylipins in the urine sample.

### 3.2. Lipid semi-quantification

The raw data files reprocessing with the Agilent MassHunter Profinder software and the subsequent data normalization and filtering allowed us to obtain a final data matrix of 315 features. From here, we obtained information regarding the abundance of each feature concerning the different lipid extraction methods. For lipid quantification, we calculated the concentration (in ppm) of the SPLASH® Lipidomix®, according to the corresponding volume added to each extracted method. After that, we calculate the lipid concentrations using the corresponding lipid species of the SPLASH® Lipidomix® (Table S1). We used the nearest lipid species to perform a semi-quantification for those lipid classes that did not have a specific internal standard (IS). For example, Cer and neutral glycosphingolipids (HexCer) were semi-quantified using the SM IS (SM 18:1_18:1 (d9)); for Car, we used the $C_{17}$-Sphinganine. The monoacylglycerides (MG) were semi-quantified using the diacylglycerol (DG) 15:0_18:1 (d7), and the FA lipid class was semi-quantified with the $d_{31}$-palmitic acid.

### 3.3. Reproducibility comparison of the one-phase and two-phase extraction protocols

Given the diversity in lipid structures and polarities, no single solvent system can extract all types of lipids without introducing biases. Rather than a pointed-out universal extraction method, we aimed to underline the characteristics of different straightforward methods for lipid extraction from urine samples. Different single-phase lipid extraction methods have been proven effective and have high lipid recovery in mammalian plasma samples [38]. Nevertheless, little is known about their suitability for lipid extraction from urine samples, a more polar matrix. As a reference extraction, we used a modification of the Matyash method [20], which was based on the original Matyash method [17] but with solvent volumes more similar to the Bligh and Dyer protocol [16]. The modified Matyash method, previously tested in plasma samples, provided higher extraction yields and recovered more peaks in both polar and non-polar fractions. It also demonstrated superior or comparable metabolite intensities to the Bligh and Dyer and original Matyash methods, making it a suitable and less toxic alternative for automated sample extraction methodologies [20].

Maintaining high analytical reproducibility during the sample preparation step is crucial for lipidomics studies, particularly when analyzing many samples to determine the lipid profile [20]. In pursuit of this goal, our primary focus was selecting the most reproducible lipid extraction strategy. When considering the entire lipidome, the MeOH:EtOH extraction method exhibited the highest reproducibility, as evidenced by the well-defined clustering of the ten replicates in the unsupervised Principal Component Analysis (PCA) (Fig. 5A). Conversely, the EtOAc:EtOH method showed a not-so-good clustering in the model.

Due to the heterogeneity of lipids, as a group, in terms of physicochemical properties, we evaluated the extraction reproducibility for each method based on individual lipid classes. The assessment involved analyzing the lipid class proportion in urine and performing semi-quantification. Next, we calculated the coefficient of variation (CV) for each feature among the ten replicates of each lipid extraction method. Using the already calculated CVs for each feature, we determined the average and standard deviation of the CVs within the same lipid class (Table 1, Fig. 5B). The resulting average CV represented the reproducibility for each lipid class. A lower average CV indicated reduced variability among the ten replicates of each lipid class for each lipid extraction protocol, signifying higher reproducibility in the sample preparation procedure.

Assessing the data shown in Table 1, we saw that, in general, the monophasic lipid extraction method MeOH:EtOH showed the highest reproducibility among all lipid classes, with the smallest average and standard deviation values. The biphasic modified Matyash method showed better average results for extracting monoacylglycerophosphocholines (LPC) (11.00 ± 7.24 SD), monoacylglycerophosphoethanolamines (LPE) (11.17 ± 4.56 SD), MG (13.73 ± 11.77 SD) and glycerophosphoinositol (PI) (6.52 ± 1.20 SD); however, the standard deviation was higher than the other methods for these sample lipid classes. The one-phase EtOAc:EtOH displayed similar reproducibility results as the MeOH:EtOH method for Cer (9.83 ± 9.94 SD), ether-linked phosphoethanolamines (PE-O) (6.76 ± 3.08 SD), ether-linked phosphocholines (PC-O) (8.11 ± 4.45 SD) and PI (8.07 ± 0.92 SD). However, the standard deviation results for Cer were very high, even higher than the corresponding average data. Analyzing the data exhibited by the MeOH:MTBE, the results relative to the Car (7.26 ± 5.65 SD), MG (17.50 ± 6.14 SD) and PI (8.11 ± 2.47 SD) were close to those portrayed in the MeOH:EtOH, for both the average and the standard deviation.

### 3.4. Biological relevance and analytical factors for each individual lipid class

Lipiduria is a characteristic feature observed in the urine of individuals diagnosed with nephrotic syndrome and other pathologies. This medical condition is characterized by elevated levels of various lipid components, including cholesterol, cholesterol ester, TG, free fatty acids (FFA), PC, PE, and phosphatidylserine (PS). These lipid substances serve as valuable diagnostic markers to identify nephrotic syndrome in patients. Hence, urinary lipid profiling has great potential in clinical diagnostics and prognostics [39].

Overall, the extraction ratio for all lipid classes was acceptable across all tested solvents. However, upon detailed and in-depth individual analysis, distinct trends were observed.

The Car exhibited an utterly different extraction rate (Fig. 3). Car are lipid derivatives consisting of a fatty acid with chain lengths from C2:0 to C26:0, connected to carnitine through an ester bond. These compounds have been widely recognized as indicators of inborn errors of metabolism and fatty acid oxidation disorders. These conditions result from defects in enzymes or transporters involved in fatty acid metabolism, leading to the accumulation of specific Car in the urine. Medium-chain acyl-CoA dehydrogenase deficiency (MCAD deficiency),

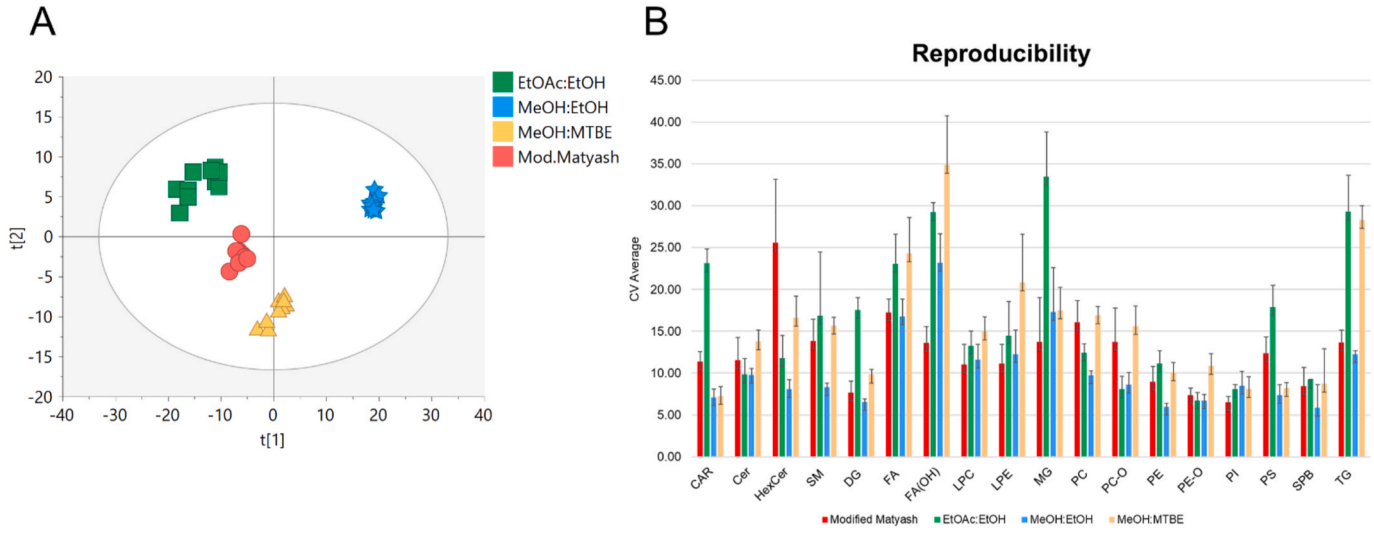


**Fig. 5.** **(A)** Unsupervised Principal Component Analysis (PCA) of the four extraction methods ($n = 10$ per method). X axis presents principal component 1 (PC1) and Y axis, PC2. The model was obtained using UV scaling ($R^2 = 0.878$). **(B)** Graphical representation of each lipid subclass CV average with the corresponding error bars (standard error of mean, SEM).

**Table 1**
The table shows the average, the standard deviation (STDEV), and the standard error of mean (SEM) of all the lipid species, classified by the lipid class and lipid extraction method applied.

| Lipid class | *Modified Matyash* | | | *EtOAc:EtOH* | | | *MeOH:EtOH* | | | *MeOH:MTBE* | | |
|---|---|---|---|---|---|---|---|---|---|---|---|---|
| | Average | STDEV | SEM | Average | STDEV | SEM | Average | STDEV | SEM | Average | STDEV | SEM |
| **Car** | 11.40 | 5.59 | 1.14 | 23.12 | 8.23 | 1.68 | 7.08 | 5.01 | 1.02 | 7.26 | 5.65 | 1.15 |
| **Cer** | 11.56 | 14.30 | 2.70 | 9.83 | 9.94 | 1.88 | 9.79 | 4.15 | 0.78 | 13.82 | 6.87 | 1.30 |
| **HexCer** | 25.58 | 20.05 | 7.58 | 11.78 | 7.10 | 2.68 | 8.10 | 2.90 | 1.10 | 16.61 | 6.89 | 2.60 |
| **SM** | 13.84 | 14.19 | 2.59 | 16.86 | 41.74 | 7.62 | 8.31 | 2.67 | 0.49 | 15.68 | 5.38 | 0.98 |
| **DG** | 7.68 | 6.67 | 1.36 | 17.57 | 7.04 | 1.44 | 6.58 | 1.54 | 0.31 | 9.82 | 2.99 | 0.61 |
| **FA** | 17.27 | 7.15 | 1.60 | 23.07 | 15.87 | 3.55 | 16.76 | 9.39 | 2.10 | 24.31 | 19.02 | 4.25 |
| **FA(OH)** | 13.63 | 6.12 | 1.93 | 29.25 | 3.41 | 1.08 | 23.20 | 10.92 | 3.45 | 34.89 | 18.52 | 5.86 |
| **LPC** | 11.00 | 7.24 | 2.41 | 13.23 | 5.33 | 1.78 | 11.61 | 5.51 | 1.84 | 14.94 | 5.38 | 1.79 |
| **LPE** | 11.17 | 4.56 | 2.28 | 14.49 | 8.12 | 4.06 | 12.26 | 5.71 | 2.85 | 20.83 | 11.50 | 5.75 |
| **MG** | 13.73 | 11.77 | 5.26 | 33.47 | 11.94 | 5.34 | 17.29 | 11.84 | 5.30 | 17.50 | 6.14 | 2.75 |
| **PC** | 16.09 | 17.12 | 2.55 | 12.43 | 7.18 | 1.07 | 9.74 | 3.63 | 0.54 | 16.90 | 6.90 | 1.03 |
| **PC-O** | 13.74 | 12.17 | 4.06 | 8.11 | 4.45 | 1.48 | 8.60 | 4.47 | 1.49 | 15.62 | 7.15 | 2.38 |
| **PE** | 8.96 | 7.03 | 1.82 | 11.17 | 5.91 | 1.53 | 5.97 | 1.67 | 0.43 | 10.09 | 4.51 | 1.16 |
| **PE-O** | 7.38 | 2.71 | 0.82 | 6.76 | 3.08 | 0.93 | 6.75 | 2.41 | 0.73 | 10.82 | 4.94 | 1.49 |
| **PI** | 6.52 | 1.20 | 0.69 | 8.07 | 0.92 | 0.53 | 8.51 | 2.98 | 1.72 | 8.11 | 2.47 | 1.43 |
| **PS** | 12.39 | 3.83 | 1.91 | 17.93 | 5.13 | 2.56 | 7.40 | 2.40 | 1.20 | 8.18 | 1.36 | 0.68 |
| **SPB** | 8.44 | 3.13 | 2.21 | 9.19 | 0.10 | 0.07 | 5.88 | 3.83 | 2.71 | 8.73 | 5.90 | 4.17 |
| **TG** | 13.69 | 11.26 | 1.43 | 29.30 | 34.16 | 4.35 | 12.26 | 3.19 | 0.41 | 28.28 | 13.48 | 1.71 |

very-long-chain acyl-CoA dehydrogenase deficiency (VLCAD deficiency), short-chain acyl-CoA dehydrogenase deficiency (SCAD deficiency), long-chain 3-hydroxy acyl-CoA dehydrogenase deficiency (LCHAD deficiency), and multiple acyl-CoA dehydrogenase deficiency (MADD) induce the urinary accumulation of specific Car, which can serve as biomarkers for diagnosing and monitoring these metabolic disorders [40]. Furthermore, there is a grade-dependent increase in urinary Car in kidney cancer patients, with strong indications that these compounds originate directly from the tumor tissue [41]. It has been suggested that augmented levels of Car in urine were associated with early kidney injury in DM patients, reflecting alterations in the β-oxidation pathway [42].

A total of 24 Car species were annotated in this study. As displayed in Fig. 6A, we included the logP values of different carnitines depending on their FA chain length. The logP value correlates with the polarity of the lipid species, influencing the extraction ratio depending on the solvent used. Smaller logP values are indicative of more polar compounds. Short-chain (C2–C5) Car, with lower logP values, had higher concentrations in the EtOAc:EtOH and MeOH:MTBE methods. Regarding the medium-chain (C6–C12), the best results were shown in the MeOH:

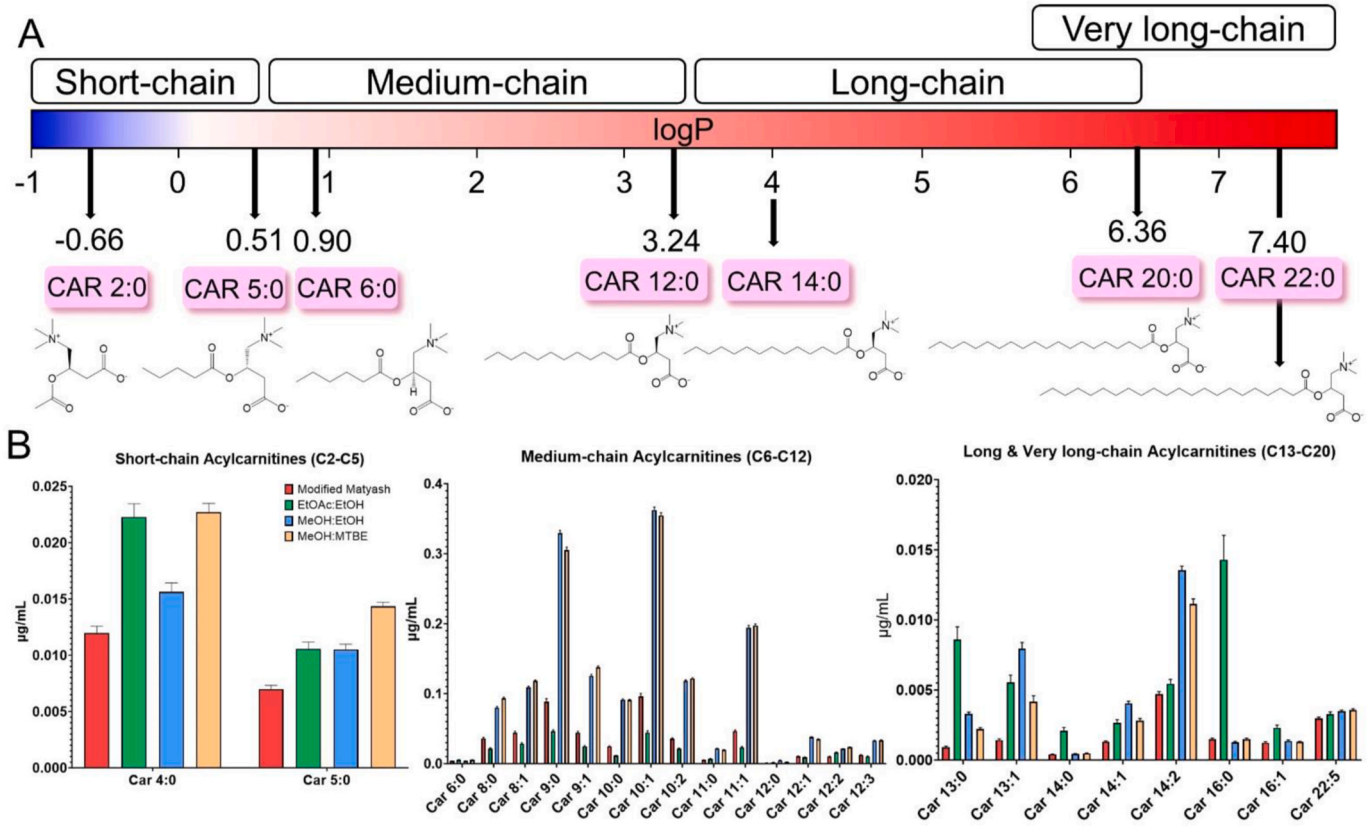


**Fig. 6. (A)** Classification of the ACar based on their acyl group lengths and logP values obtained from LIPIDMAPS. **(B)** Bar plots of ACar divided by the acyl chain length, which impacted the solvent combination preference and, therefore, their extraction rate. The error bars represent the standard error of mean (SEM).

EtOH and MeOH:MTBE extraction methods. Finally, the higher extraction rates for long-chain (C13–C20) Car corresponded to EtOAc:EtOH followed by the MeOH:EtOH. However, when considering the reproducibility of each extraction protocol, the MeOH:EtOH mixture displayed the lower CV(%) (Fig. 5B).

Recently, changes in the urinary levels of glycerophospholipids and sphingolipids were detected in COVID-19 patients, undergoing distinct changes based on disease severity and infection progression, indicating their potential relevance in identifying kidney alterations associated with COVID-19 [43]. Additionally, specific PE and PC lipid species are detected in urine after cadmium exposure, which has been linked to various health problems such as circulatory toxicity, renal damage, central and peripheral neurotoxicity, carcinogenesis, pulmonary disease, hyperkeratosis, and acanthosis in the skin [44]. Additionally, GPs in urine play a role in kidney stone formation, and their presence may indicate renal epithelial cell membrane injury [45]. Animal studies have further demonstrated that phospholipiduria can occur due to injury to renal epithelial cell membranes following exposure to specific drugs or

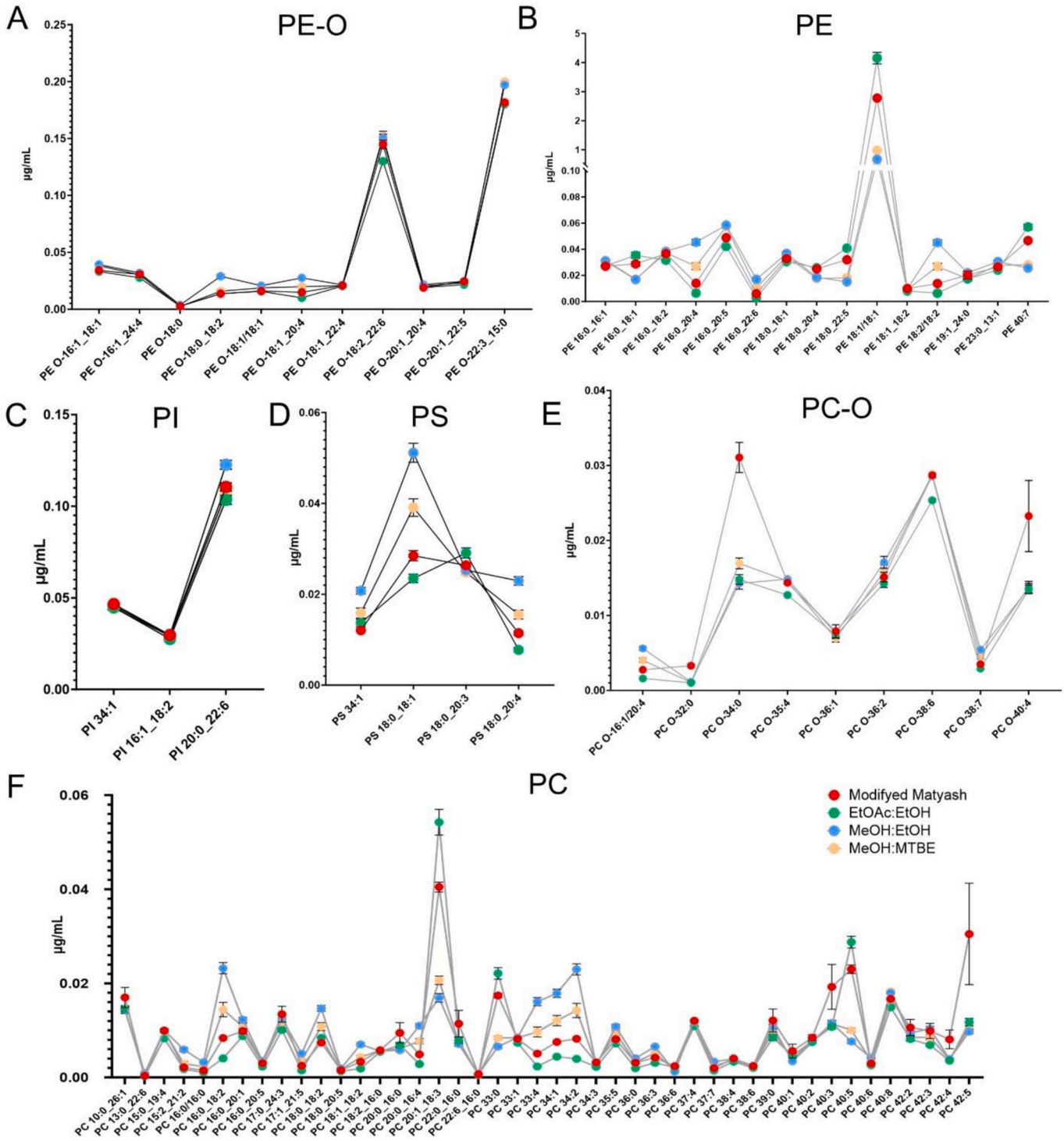


**Fig. 7.** Graphical representation of **(A)** PE-O, **(B)** PE, **(C)** PI, **(D)** PS, **(E)** PC-O, and **(F)** PC plotted against their respective concentrations in µg/mL, obtained through each extraction protocol. The error bars represent the standard error of mean (SEM).

toxic substances [46]. Furthermore, both PE and PS are observable in the urine of patients with metabolic disorders stemming from mitochondrial DNA dysfunction [47]. Consequently, the measurement of GPs in urine is crucial due to their potential as biomarkers for various health conditions.

Polar monoacylglycerophospholipids (LGP), including LPC and LPE, exhibited higher concentrations when extracted with the Modified Matyash method and the MeOH:EtOH solvent combination (Figs. S1A and S1B). The presence of polar solvents ($H_2O$ and MeOH) during the extraction process favored the higher extraction rates for these lipids [48]. Interestingly, GP showed a slightly different solvent preference than LGP. PE-O demonstrated the highest extraction rate with the MeOH:EtOH combination, particularly in the C18 species (Fig. 7A). However, for the C18:0 and C18:1 series of PE lipids, the modified Matyash and EtOAc:EtOH methods exhibited higher concentrations (Fig. 7B). PI did not exhibit significant differences in extraction rates among the four methods, indicating a consistent extraction efficiency for this lipid class (Fig. 7C). On the other hand, PS lipids showed a preference for the MeOH:EtOH method, resulting in higher concentrations (Fig. 7D). The extraction rates of PC-O were particularly noteworthy. The modified Matyash method showed a higher extraction rate for PC-O lipids, although this rate decreased in the case of polyunsaturated species (Fig. 7E). This observation may be attributed to the increased polarity of polyunsaturated lipids due to a higher number of double bonds, making solvent combinations like MeOH:MTBE more efficient in extracting these species. Within the PC lipid subclass, medium-chain length PC lipids demonstrated higher extraction rates with the MeOH:EtOH combination, while long or very long-chain PC lipids exhibited a higher affinity for the modified Matyash extraction method (Fig. 7F).

In recent years, the role of SP in several pathologies, such as inflammatory diseases, cancer, Alzheimer's and Parkinson's diseases and lysosomal storage disorders [49] has been pointed out. LC-MS analysis of urinary SP has been previously employed to study stage 3 diabetic kidney disease (DKD) patients, showing an increment in the levels of different Cer species, which correlated with proteinuria and the severity of DKD [50]. Sphingolipids play an essential role in maintaining renal function, where an increase in the Cer levels leads to podocyte damage and consequent renal failure [51]. Furthermore, urinary SP were also studied in patients with lupus nephritis, showing a significant increase in glycosphingolipid levels [52]. Alterations in the urinary sphingolipid levels were also reported in aspirin-exacerbated respiratory disease (AERD), specifically for urinary sphingosine [53]. Paying attention to the SP, Cer generally did not exhibit differences between the extraction rates of the solvent combinations (Fig. S1C). However, specific Cer species, such as Cer 18:0; 2O/18:0, 18:0; 2O/20:0, 18:1; 2O/18:0, 18:1; 2O/20:0, and 18:2; 2O/18:0, displayed a slight increase in

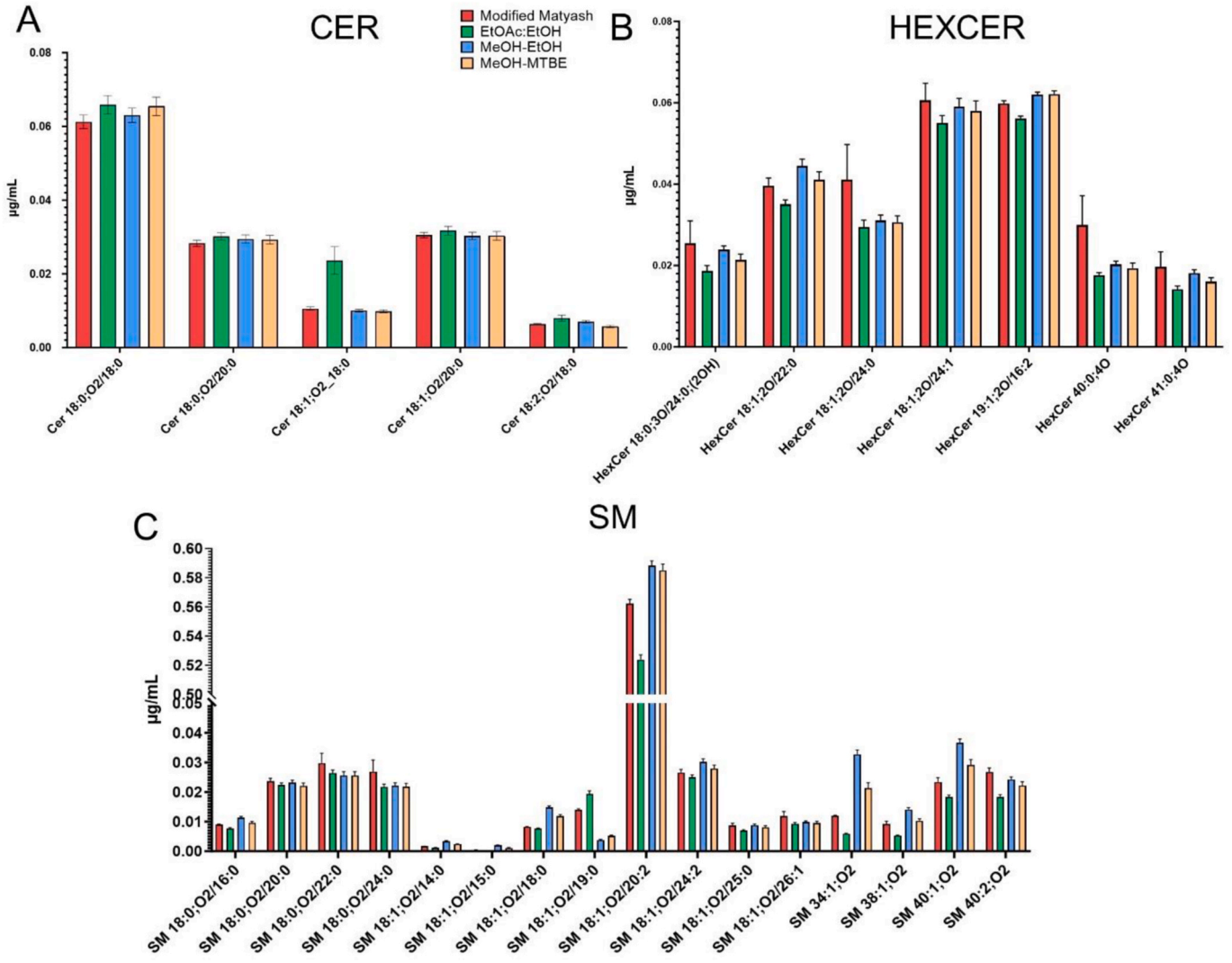


**Fig. 8.** Bar plots of **(A)** Cer, **(B)** HexCer, and **(C)** SM plotted against their respective concentrations in µg/mL, acquired through each extraction protocol. The error bars represent the standard error of mean (SEM).

concentrations when extracted using the EtOAc:EtOH method (Fig. 8A). This indicates that the EtOAc:EtOH method might be more suitable for extracting these particular ceramide species due to potential differences in their polarity and other physicochemical properties compared to other ceramides. Next, HexCer showed better extraction rate results using the modified Matyash method (Fig. 8B). Interestingly, this result did not align with the findings from its precursor, indicating that the polarity and other physicochemical properties of these lipid subclasses might influence the extraction preferences. For SM, lipids corresponding to the C18:0 series showed better extraction with the modified Matyash method, while lipids from the C18:1 series were more efficiently extracted using the MeOH:EtOH solvent combination (Fig. 8C). Further information about the lipid extraction rate of other SM can be found in Fig. S1D.

As was already mentioned before, urinary metabolites are influenced by different factors such as diet, exercise, drugs, sex, and age, leading to a lipidomic profile that reflects the metabolic and pathophysiological conditions of an individual. Different studies have revealed alterations in urine molecules relevant to pathways of glycerolipid and glycerophospholipid metabolism, thermogenesis, and caffeine metabolism, associated with Alzheimer's disease, which also produce metabolic changes in fatty acids and amino acids due to the implication of these metabolites in the biosynthesis pathway of GL and GP [54]. In our case, regarding GLs, which are low-polar compounds, MG exhibited higher concentrations in the EtOAc:EtOH extraction method, followed by the modified Matyash method, as illustrated in Fig. 9A. Conversely, DG and TG had higher concentrations in the modified Matyash and MeOH:EtOH methods, respectively (Fig. 9B). However, there were some exceptions. The highest concentrations were reached with the EtOAc:EtOH method for TG 54:3, TG 54:4, TG 54:5, and TG 54:6. This could be attributed to the low polarity of these compounds, where the EtOAc, being less polar than EtOH, likely enhanced their extraction (Fig. 9C). It's essential to note that the error bars, in this case, were relatively long, suggesting a degree of variability in the data.

Finally, among the FFA, the extraction method displaying the highest concentrations was the EtOAc:EtOH (Figs. S1E and S1F). However, it must be kept in mind that this extraction protocol showed the highest analytical variability (Fig. 5B).

A crucial factor when selecting the extraction protocol could be sample availability. In this regard, the EtOAc:EtOH method emerged as the most efficient for small sample volumes, requiring only 10 μL of urine. For instance, collecting urine samples from small animals like mice can be challenging due to the animal's small size and instinct to urinate frequently and in small amounts. In these cases, we must consider the potential sample contamination, the welfare and stress levels of the animals, and the ease of the collection procedure [55]. Similarly, collecting urine from infants with minimal bladder capacity, resulting in frequent voiding and small volumes, poses its own set of challenges [56]. However, it's important to note that the reproducibility of this method is lower compared to the other two monophasic methods, such as the modified Matyash, as illustrated in Fig. 5B. The modified Matyash method required only 20 μL of urine and yielded a wide range of lipid classes in the urine lipidic profile. However, it's important to acknowledge that this extraction method requires more sample handling and is time-consuming, potentially leading to procedural errors and might reduce result reproducibility (Fig. 5B). Among the monophasic

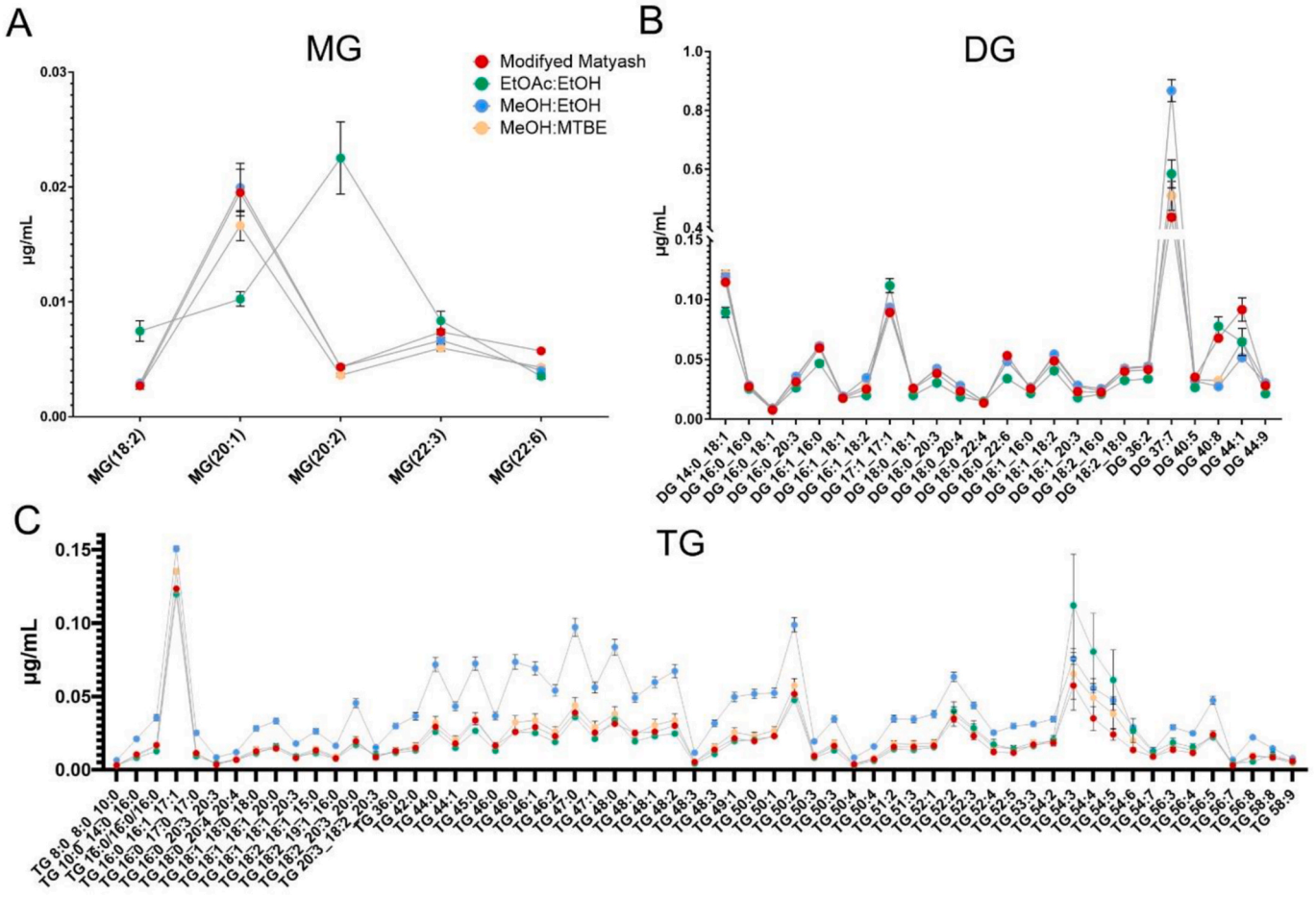


**Fig. 9.** Graphical representation of **(A)** MG, **(B)** DG, and **(C)** TG plotted against their respective concentrations in μg/mL, obtained through each extraction protocol. The error bars represent the standard error of mean (SEM).

extraction methods, the MeOH:EtOH protocol requires 100 μL of urine, which might be impractical for studies with limited sample availability or those intending to perform a multiplatform analysis. Nonetheless, this method boasts the advantage of having the lowest sample-to-solvent ratio among all the tested methods in our study, contributing to enhanced reproducibility (Fig. 5B). Finally, the MeOH:MTBE method required 50 μL of the urine sample. This solvent combination proves highly effective for extracting non-polar lipid compounds. However, it's worth noting that as a solvent, MTBE may introduce plasticizers from the Eppendorf tubes, potentially contaminating the sample.

## 4. Conclusions

Monophasic methods have gained popularity due to their simultaneous analysis of polar and nonpolar metabolites and their simplicity. However, it is evident that no single solvent system can universally extract all lipid types without potentially introducing some bias. Rather than pursuing a one-size-fits-all extraction method, our objective was to identify a straightforward approach suitable for high-throughput lipid extraction from urine samples. Maintaining analytical reproducibility during sample preparation is paramount for untargeted lipidomics studies, especially when analyzing a large number of samples to establish lipid profiles. Our primary focus was on selecting the most reproducible lipid extraction strategy. When considering the entire lipidome, the MeOH:EtOH extraction method displayed the highest reproducibility, as evident from the well-defined clustering of replicates in the PCA. Conversely, the EtOAc:EtOH method exhibited the lowest reproducibility, with replicates showing poor clustering.

To account for the heterogeneous nature of lipids, we evaluated the extraction reproducibility for individual lipid classes. It is essential to emphasize that in untargeted analysis, samples are compared under identical conditions to unveil biological alterations related to the pathology under study. Therefore, the reproducibility of the extraction procedure is the key parameter. Upon analyzing the data, we observed that, in general, the monophasic MeOH:EtOH extraction method exhibited the highest reproducibility across all lipid classes.

The biphasic-modified Matyash method also showed favorable results for certain lipid classes but exhibited higher standard deviations. The one-phase EtOAc:EtOH method yielded reproducibility results similar to the MeOH:EtOH method for several lipid classes but showed higher standard deviation values for some others. Furthermore, the biological relevance and analytical significance of specific lipid classes, such as carnitines, glycerophospholipids, sphingolipids, and free fatty acids, in various health conditions and diseases is also critical. Consequently, understanding the extraction preferences of these lipid classes is crucial to making informed choices in lipidomics studies.

In summary, our study provides valuable insights into selecting an appropriate lipid extraction method for urine samples, considering the specific requirements of each study, sample availability, and the trade-off between reproducibility and extraction efficiency. This information will aid researchers in optimizing their lipidomics workflows when using urine samples and ultimately enhance the reliability of lipid profile analysis in diverse research and clinical applications.

## Funding

This research was funded by the Ministry of Science and Innovation of Spain (MCIN) through MCIN/AEI/10.13039/501100011033 and ERDF A way of making Europe, under grant number PID 2021-122490NB-I00, and the Autonomous Community of Madrid INNOREN-CM S2022/BMD-7221.

## CRediT authorship contribution statement

**Belen Fernandez Requena:** Data curation, Investigation, Software, Writing – original draft. **Carolina Gonzalez-Riano:** Conceptualization, Investigation, Methodology, Supervision, Writing – original draft. **Coral Barbas:** Conceptualization, Funding acquisition, Project administration, Resources, Supervision, Writing – review & editing.

## Declaration of competing interest

The authors declare the following financial interests/personal relationships which may be considered as potential competing interests: Dr. Coral Barbas reports financial support was provided by Spain Ministry of Science and Innovation.

## Data availability

Data will be made available on request.

## Acknowledgements

The authors offer special thanks to Vanesa Alonso for her technical assistance and advice.

## Appendix A. Supplementary data

Supplementary data to this article can be found online at https://doi.org/10.1016/j.aca.2024.342433.

## References

[1] X. Li, K. Nakayama, T. Goto, S. Akamatsu, K. Shimizu, O. Ogawa, T. Inoue, Comparative evaluation of the extraction and analysis of urinary phospholipids and lysophospholipids using MALDI-TOF/MS, Chem. Phys. Lipids 223 (2019) 104787.
[2] M. Cala, J. Aldana, J. Sánchez, J. Guio, R.J. Meesters, Urinary metabolite and lipid alterations in Colombian Hispanic women with breast cancer: a pilot study, J. Pharmaceut. Biomed. Anal. 152 (2018) 234–241.
[3] T. Xu, C. Hu, Q. Xuan, G. Xu, Recent advances in analytical strategies for mass spectrometry-based lipidomics, Anal. Chim. Acta 1137 (2020) 156–169.
[4] J. Graessler, C. Mehnert, K. Schulte, S. Bergmann, S. Strauss, T. Bornstein, J. Licinio, M. Wong, A. Birkenfeld, S. Bornstein, Urinary Lipidomics: evidence for multiple sources and sexual dimorphism in healthy individuals, Pharmacogenomics J. 18 (2018) 331–339.
[5] N. Nagata, Y. Hamasaki, S. Inagaki, T. Nakamura, D. Horikami, K. Yamamoto-Hanada, Y. Inuzuka, T. Shimosawa, K. Kobayashi, M. Narita, Urinary lipid profile of atopic dermatitis in murine model and human patients, Faseb. J. 35 (2021) e21949.
[6] K. Jurowski, K. Kochan, J. Walczak, M. Barańska, W. Piekoszewski, B. Buszewski, Analytical techniques in lipidomics: state of the art, Crit. Rev. Anal. Chem. 47 (2017) 418–437.
[7] S.K. Byeon, J.Y. Kim, J.-S. Lee, M.H. Moon, Variations in plasma and urinary lipids in response to enzyme replacement therapy for Fabry disease patients by nanoflow UPLC-ESI-MS/MS, Anal. Bioanal. Chem. 408 (2016) 2265–2274.
[8] N. Vinayavekhin, A. Saghatelian, Untargeted metabolomics, Curr. Protoc. Mol. Biol. 90 (2010) 30, 31. 31-30.31. 24.
[9] T. Cajka, O. Fiehn, Toward merging untargeted and targeted methods in mass spectrometry-based metabolomics and lipidomics, Anal. Chem. 88 (2016) 524–545.
[10] T. Züllig, M. Trötzmüller, H.C. Köfeler, Lipidomics from sample preparation to data analysis: a primer, Anal. Bioanal. Chem. 412 (2020) 2191–2209.
[11] D.Y. Bang, S.K. Byeon, M.H. Moon, Rapid and simple extraction of lipids from blood plasma and urine for liquid chromatography-tandem mass spectrometry, J. Chromatogr. A 1331 (2014) 19–26.
[12] S.K. Byeon, J.Y. Lee, J.-S. Lee, M.H. Moon, Lipidomic profiling of plasma and urine from patients with Gaucher disease during enzyme replacement therapy by nanoflow liquid chromatography–tandem mass spectrometry, J. Chromatogr. A 1381 (2015) 132–139.
[13] F. Wei, S. Lamichhane, M. Orešič, T. Hyötyläinen, Lipidomes in health and disease: analytical strategies and considerations, TrAC, Trends Anal. Chem. 120 (2019) 115664.
[14] S.K. Byeon, J.Y. Lee, M.H. Moon, Optimized extraction of phospholipids and lysophospholipids for nanoflow liquid chromatography-electrospray ionization-tandem mass spectrometry, Analyst 137 (2012) 451–458.
[15] J. Folch, M. Lees, G.H. Sloane Stanley, A simple method for the isolation and purification of total lipids from animal tissues, J. Biol. Chem. 226 (1957) 497–509.
[16] E.G. Bligh, W.J. Dyer, A rapid method of total lipid extraction and purification, Can. J. Biochem. Physiol. 37 (1959) 911–917.
[17] V. Matyash, G. Liebisch, T.V. Kurzchalia, A. Shevchenko, D. Schwudke, Lipid extraction by methyl-tert-butyl ether for high-throughput lipidomics* s, JLR (J. Lipid Res.) 49 (2008) 1137–1146.
[18] A. Gil, W. Zhang, J.C. Wolters, H. Permentier, T. Boer, P. Horvatovich, M. R. Heiner-Fokkema, D.-J. Reijngoud, R. Bischoff, One-vs two-phase extraction: re-

evaluation of sample preparation procedures for untargeted lipidomics in plasma samples, Anal. Bioanal. Chem. 410 (2018) 5859–5870.
[19] M. Horing, C. Stieglmeier, K. Schnabel, T. Hallmark, K. Ekroos, R. Burkhardt, G. Liebisch, Benchmarking one-phase lipid extractions for plasma lipidomics, Anal. Chem. 94 (2022) 12292–12296.
[20] J. Sostare, R. Di Guida, J. Kirwan, K. Chalal, E. Palmer, W.B. Dunn, M.R. Viant, Comparison of modified Matyash method to conventional solvent systems for polar metabolite and lipid extractions, Anal. Chim. Acta 1037 (2018) 301–315.
[21] C. Gonzalez-Riano, A. Gradillas, C. Barbas, Exploiting the formation of adducts in mobile phases with ammonium fluoride for the enhancement of annotation in liquid chromatography-high resolution mass spectrometry based lipidomics, Journal of Chromatography Open 1 (2021) 100018.
[22] B. Fernández Requena, S. Nadeem, V.P. Reddy, V. Naidoo, J.N. Glasgow, A. J. Steyn, C. Barbas, C. Gonzalez-Riano, LiLA: lipid lung-based ATLAS built through a comprehensive workflow designed for an accurate lipid annotation, Commun. Biol. 7 (2024) 45.
[23] A. Gil-de-la-Fuente, J. Godzien, S. Saugar, R. Garcia-Carmona, H. Badran, D. S. Wishart, C. Barbas, A. Otero, CEU mass mediator 3.0: a metabolite annotation tool, J. Proteome Res. 18 (2018) 797–802.
[24] E.N. Pieke, K. Granby, X. Trier, J. Smedsgaard, A framework to estimate concentrations of potentially unknown substances by semi-quantification in liquid chromatography electrospray ionization mass spectrometry, Anal. Chim. Acta 975 (2017) 30–41.
[25] J.P. Koelmel, X. Li, S.M. Stow, M.J. Sartain, A. Murali, R. Kemperman, H. Tsugawa, M. Takahashi, V. Vasiliou, J.A. Bowden, Lipid annotator: towards accurate annotation in non-targeted liquid chromatography high-resolution tandem mass spectrometry (LC-HRMS/MS) lipidomics using a rapid and user-friendly software, Metabolites 10 (2020) 101.
[26] H. Tsugawa, K. Ikeda, M. Takahashi, A. Satoh, Y. Mori, H. Uchino, N. Okahashi, Y. Yamada, I. Tada, P. Bonini, A lipidome atlas in MS-DIAL 4, Nat. Biotechnol. 38 (2020) 1159–1163.
[27] Z. Ni, G. Angelidou, M. Lange, R. Hoffmann, M. Fedorova, LipidHunter identifies phospholipids by high-throughput processing of LC-MS and shotgun lipidomics datasets, Anal. Chem. 89 (2017) 8800–8807.
[28] M.I. Alcoriza-Balaguer, J.C. Garcia-Canaveras, A.n. López, I. Conde, O. Juan, J. n. Carretero, A. Lahoz, LipidMS: an R package for lipid annotation in untargeted liquid chromatography-data independent acquisition-mass spectrometry lipidomics, Anal. Chem. 91 (2018) 836–845.
[29] M.I. Alcoriza-Balaguer, J.C. García-Cañaveras, F.J. Ripoll-Esteve, M. Roca, A. Lahoz, LipidMS 3.0: an R-package and a web-based tool for LC-MS/MS data processing and lipid annotation, Bioinformatics 38 (2022) 4826–4828.
[30] G.a. Graca, Y. Cai, C.-H.E. Lau, P.A. Vorkas, M.R. Lewis, E.J. Want, D. Herrington, T.M. Ebbels, Automated annotation of untargeted all-ion fragmentation LC–MS metabolomics data with MetaboAnnotatoR, Anal. Chem. 94 (2022) 3446–3455.
[31] A. Criscuolo, P. Nepachalovich, D.F. Garcia-del Rio, M. Lange, Z. Ni, M. Baroni, G. Cruciani, L. Goracci, M. Blüher, M. Fedorova, Analytical and computational workflow for in-depth analysis of oxidized complex lipids in blood plasma, Nat. Commun. 13 (2022) 6547.
[32] G. Liebisch, E. Fahy, J. Aoki, E.A. Dennis, T. Durand, C.S. Ejsing, M. Fedorova, I. Feussner, W.J. Griffiths, H. Köfeler, Update on LIPID MAPS classification, nomenclature, and shorthand notation for MS-derived lipid structures, JLR (J. Lipid Res.) 61 (2020) 1539–1555.
[33] K. Okemoto, K. Maekawa, Y. Tajima, M. Tohkin, Y. Saito, Cross-classification of human urinary lipidome by sex, age, and body mass index, PLoS One 11 (2016) e0168188.
[34] P. Tipthara, V. Thongboonkerd, Differential human urinary lipid profiles using various lipid-extraction protocols: MALDI-TOF and LIFT-TOF/TOF analyses, Sci. Rep. 6 (2016) 33756.
[35] C. Gómez, C. Gonzalez-Riano, C. Barbas, J. Kolmert, M.H. Ryu, C. Carlsten, S.-E. Dahlén, C.E. Wheelock, Quantitative metabolic profiling of urinary eicosanoids for clinical phenotyping, JLR (J. Lipid Res.) 60 (2019) 1164–1173.
[36] L. Janssen, Isoprostanes: generation, pharmacology, and roles in free-radical-mediated effects in the lung, Pulm. Pharmacol. Therapeut. 13 (2000) 149–155.
[37] A. Sasaki, H. Fukuda, N. Shiida, N. Tanaka, A. Furugen, J. Ogura, S. Shuto, N. Mano, H. Yamaguchi, Determination of ω-6 and ω-3 PUFA metabolites in human urine samples using UPLC/MS/MS, Anal. Bioanal. Chem. 407 (2015) 1625–1639.
[38] J. Medina, R. Borreggine, T. Teav, L. Gao, S. Ji, J. Carrard, C. Jones, N. Blomberg, M. Jech, A. Atkins, Omic-scale high-throughput quantitative LC–MS/MS approach for circulatory lipid phenotyping in clinical research, Anal. Chem. 95 (2023) 3168–3179.
[39] C. Macé, S.S. Chugh, Nephrotic Syndrome: Components, Connections, and Angiopoietin-like 4-related Therapeutics..
[40] J.J. Pitt, M. Eggington, S.G. Kahler, Comprehensive screening of urine samples for inborn errors of metabolism by electrospray tandem mass spectrometry, Clin. Chem. 48 (2002) 1970–1980.
[41] S. Ganti, S.L. Taylor, K. Kim, C.L. Hoppel, L. Guo, J. Yang, C. Evans, R.H. Weiss, Urinary acylcarnitines are altered in human kidney cancer, Int. J. Cancer 130 (2012) 2791–2800.
[42] F. Van der Kloet, F. Tempels, N. Ismail, R. Van der Heijden, P. Kasper, M. Rojas-Cherto, R. Van Doorn, G. Spijksma, M. Koek, J. Van Der Greef, Discovery of early-stage biomarkers for diabetic kidney disease using ms-based metabolomics (FinnDiane study), Metabolomics 8 (2012) 109–119.
[43] M. Kurano, D. Jubishi, K. Okamoto, H. Hashimoto, E. Sakai, Y. Morita, D. Saigusa, K. Kano, J. Aoki, S. Harada, Dynamic modulations of urinary sphingolipid and glycerophospholipid levels in COVID-19 and correlations with COVID-19-associated kidney injuries, J. Biomed. Sci. 29 (2022) 1–18.
[44] H. Hong, J. Xu, H. He, X. Wang, L. Yang, P. Deng, L. Yang, M. Tan, J. Zhang, Y. Xu, Cadmium perturbed metabolomic signature in pancreatic beta cells correlates with disturbed metabolite profile in human urine, Environ. Int. 161 (2022) 107139.
[45] C. Boonla, P. Youngjermchan, S. Pumpaisanchai, K. Tungsanga, P. Tosukhowong, Lithogenic activity and clinical relevance of lipids extracted from urines and stones of nephrolithiasis patients, Urol. Res. 39 (2011) 9–19.
[46] C. Josepovitz, R. Levine, B. Lane, G. Kaloyanides, Contrasting effects of gentamicin and mercuric chloride on urinary excretion of enzymes and phospholipids in the rat, Laboratory Investigation, a Journal of Technical Methods and Pathology 52 (1985) 375–386.
[47] E.-i. Uyama, Y. Kutsukake, A. Hara, K.-i. Uemura, M. Uchino, S. Mita, M. Ando, T. Taketomi, Abnormal excretion of urinary phospholipids and sulfatide in patients with mitochondrial encephalomyopathies, Biochem. Biophys. Res. Commun. 194 (1993) 266–273.
[48] N.V. X.4, 2023.
[49] B.M. Quinville, N.M. Deschenes, A.E. Ryckman, J.S. Walia, A comprehensive review: sphingolipid metabolism and implications of disruption in sphingolipid homeostasis, Int. J. Mol. Sci. 22 (2021) 5793.
[50] Y. Morita, M.A.-O. Kurano, E. Sakai, T. Nishikawa, M. Nishikawa, M. Sawabe, J. Aoki, Y. Yatomi, Analysis of Urinary Sphingolipids Using Liquid Chromatography-Tandem Mass Spectrometry in Diabetic Nephropathy..
[51] S.K. Mallela, S. Merscher, A. Fornoni, Implications of sphingolipid metabolites in kidney diseases, Int. J. Mol. Sci. 23 (2022) 4244.
[52] O.C. Harden, S.M. Hammad, Sphingolipids and diagnosis, prognosis, and organ damage in systemic lupus erythematosus, Front. Immunol. 11 (2020) 586737.
[53] H.K.T. Trinh, S.-C. Kim, K. Cho, S.-J. Kim, G.-Y. Ban, H.-J. Yoo, J.-Y. Cho, H.-S. Park, S.-H. Kim, Exploration of the sphingolipid metabolite, sphingosine-1-phosphate and sphingosine, as novel biomarkers for aspirin-exacerbated respiratory disease, Sci. Rep. 6 (2016) 36599.
[54] Y. Watanabe, K. Kasuga, T. Tokutake, K. Kitamura, T. Ikeuchi, K. Nakamura, Alterations in glycerolipid and fatty acid metabolic pathways in Alzheimer's disease identified by urinary metabolic profiling: a pilot study, Front. Neurol. 12 (2021) 719159.
[55] B.T. Kurien, N.E. Everds, R.H. Scofield, Experimental animal urine collection: a review, Lab. Anim 38 (2004) 333–361.
[56] J. Kaufman, M. Temple-Smith, L. Sanci, Urine sample collection from young pre-continent children: common methods and the new Quick-Wee technique, Br. J. Gen. Pract. 70 (2020) 42–43.